ANR report, task 1: cosmic tests

Vladislav Balagura, LLR, balagura@llr.in2p3.fr,
June 2014

1 Introduction

Before 2013 the cosmic running was almost impossible because of high noises in the SKIROC power lines. They caused retriggerings when the noise in one bunch crossing (BX) initiated a series of triggers in BX+1, BX+2, ... Most of the time, all 15 memory slots in the SKIROC chip were exhausted very fast, before the first muon arrived. The low cosmic rate could not compete with such high rate noises.

In 2013 the decoupling capacitors in the power lines significantly improved the situation. The first successful cosmic runs have been taken in May 2013. After that they have been taken routinely and have been used for various calibration and debugging purposes. All cosmic runs have been taken in LLR.

To increase the data collection efficiency, the spill duty cycle was increased as much as possible. The CCC rotating switch was set to "SPILL" mode, meaning that the data taking was controlled only by the spill signal (note, hits were recorded when the signal was low). With the typical spill frequency around 5 Hz and the idle time of 30 msec, the collection efficiency is $170/200 = 85\%$. 30 msec was found to be almost always sufficient for the subsequent readout of all recorded hits in the slab. During this time the slab is not sensitive to cosmic particles, it only processes already recorded hits. Note, that in the charge injection tests it is checked, that in the most "busy" case when all 15 memories of all chips are fired in the spill, the necessary idle spill time (ie. readout time) is between 50 and 55 msec. Therefore, in such "most busy" conditions 55 msec is both required and sufficient. In cosmic running the data traffic is lower, so that 30 msec is almost always sufficient. In fact, there is still some negligible fraction of events when readout takes longer. For such spills the data format is corrupted: the header of the next spill (with the number $N + 1$) appears before the trailer of the current spill (N). Such spills are simply removed by the software and are not analyzed.

The cosmic rate was lower than expected until January 2014 when the bug was finally found and fixed. It limited the duration of data taking to 5 first msec in the spill, instead of expected 170 msec in the above settings. In fact, 5 msec limitation was introduced in DIF firmware to limit the discharge of big

(400 mF) capacitor in power pulsing mode. This capacitor supplies the power current for all front-end electronics during the spill. According to maximal discharge specifications of the capacitor and the current in the final system, 5 msec limitation was chosen for safety reasons. In the small prototype like existing short slabs, the discharge is much slower. In addition, in the prototypes used up to now in the cosmic tests the capacitor is not disconnected from the power line, so the current is supplied also by the power source. Therefore, it was safe to remove the 5 msec limitation. This was done in the DIF firmware for the so-called "Beam Test" (BT) mode which should only be used for cosmic tests. In XML configuration file used in CALICOES readout software it is selected by the following line

```
<param name="dif_mode">BT</param>
```

After fixing the limitation above, the cosmic rate is slightly less than 2 Hz per slab. It allows to calibrate all slabs with the statistical accuracy of $\sim 3\%$ per channel in 24 hours, see later.

The noisy channel masking for all cosmic runs was performed with an automatic procedure described in the next section. All trigger thresholds in all chips were set the same, this significantly simplified the following analysis.

2 Automatic masking algorithm

In the beginning, all trigger thresholds are set at a very high level. Optionally, the channels connected to 2 or 4 silicon sensor pixels are masked because they always have higher noises. Then, the thresholds are gradually decreased. At each step the data is taken during three seconds with the cosmic spill settings. If three or more hits are detected in the same channel, it is automatically masked. Note, that the probability to have even two cosmic hits in the same pixel in three seconds is negligible, so three hits may be produced only by noise.

In the retriggered events in the BX+1, ... bunch crossings, many hits may be fired at once. We are interested only in the noisy channels in the first BX, which initiated the hit avalanche. By masking the seed, the avalanche may be avoided. Therefore, all retriggers are removed from the analysis and only the first BX is considered. In addition, any event with 32 or more hits is also removed.

If no noisy hits are found at a given trigger threshold, the threshold is decreased. Otherwise, all found noisy channels are masked and three seconds running at the same threshold is repeated. Maximally two iterations at any threshold are allowed, ie. after the second iteration the threshold is decreased regardless of whether new noisy channels are found. The described algorithm logic was chosen empirically, it provides sufficiently quiet environment.

Alternative solution to find noisy channels is to measure full S-curves of threshold – firing fraction dependence for every channel. The rest of the channels should be masked and disabled, otherwise at low thresholds the events are completely dominated by retriggerings and normal operation is not possible.

Precise per channel S-curves provide a lot of information, but their determination is slow, as the threshold scan is essentially multiplied by the total number of channels. With the specially written automatic masking – unmasking procedure per channel, an estimated duration for one slab is about one night.

The procedure described above process all channels in parallel at the same time. Currently, it takes less than 5 minutes. At any given threshold it determines the required masking, making a system more or less quiet. In the end, after setting the final threshold, the system is able to take cosmic at a rate of about 2 Hz. The noise rate is sufficiently small compared to that, so that the fraction of events when SKIROC memory is full due to noise is negligible.

Note, that in the beam test in February 2013 it was found that the noise pattern was changing on the time scale of one hour. After that, in spring 2013, the decoupling capacitors in the power lines were implemented for filtering the power noise. This significantly reduced the overall noises. There were two cosmic runs for about a week, in May 2013 and in Dec 2013, and the noise pattern during the whole week was sufficiently stable compared to what was determined from the automatic masking procedure just before the runs. No one noisy channel appeared which would exhaust the SKIROC memory.

3 First test in May 2013

The first cosmic runs have been taken in May 2013, the results have been reported at ILD ECAL meeting in Paris, LPNHE, on June 3, 2013 ("Silicon-Tungsten ECAL, tests and plans", the first presentation in
`https://agenda.linearcollider.org/conferenceDisplay.py?confId=6036`,
pp. 16-20).

In total 5 slabs have been analyzed. Four of them (#2,6,7,10) already had decoupling capacitors in the power lines which helped against the noises. In December 2012 a bug was discovered in front-end PCB (FEV8): one analog power line was connected to a digital power. Clearly, this increased the noise. To estimate the importance of the effect, in the 5th slab (#9) this bug was fixed, but the decoupling capacitors were not added. Fig. 1 shows the accumulated during one week cosmic signal in every chip as a table of 5 slabs (rows), each with 4 chips (columns). Note the logarithmic scale. As one can see, the behaviour of slab #9 was improved by fixing the FEV8 bug, but the decoupling capacitors helped more, even in the presence of this bug. Note, that in the next versions of FEV both this bug is fixed and the decoupling capacitors are implemented by default.

The fraction of channels masked by the automatic procedure was 5.1% in addition to 9.4% of channels masekd by default because they were connected to 2 or 4 pixels (note, there will be no such channels in the next FEV). The threshold was slightly higher than 0.5 MIP (35 ADC counts in the plots). The SKIROC gain was 5 times larger than the lowest gain which is foreseen for a nominal operation. The gain is inversely proportional to a configurable internal SKIROC capacitor. In this case it was 1.2 pF, the lowest gain corresponds to

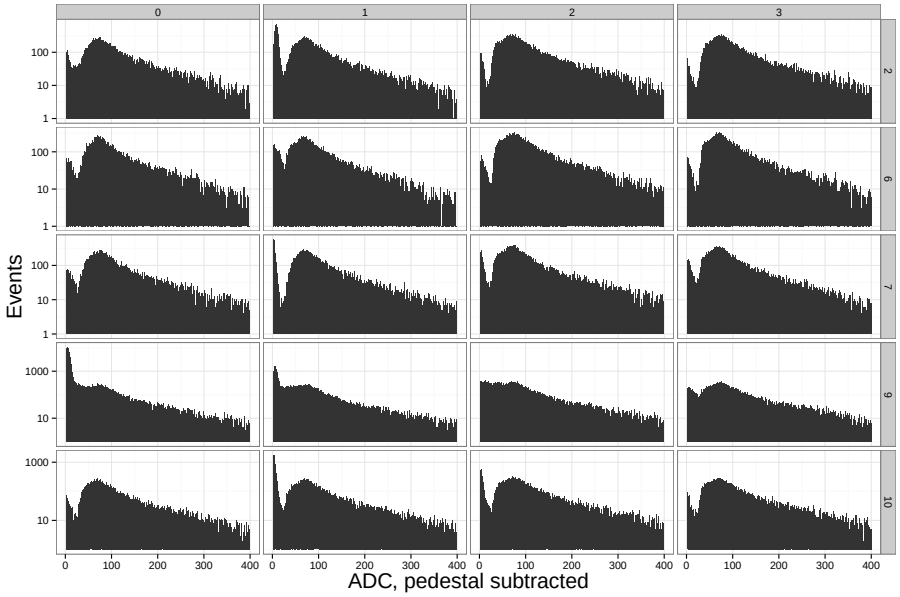

Figure 1: Accumulated during a week in May 2013 cosmic signals per chip for 5 slabs. Pedestals are subtracted. Note the logarithmic scale. All slabs had decoupling capacitors in the power lines except slab #9, where, instead, the FEV8 bug described in the text was fixed. The statistics was low due to a data taking limit of 5 msec per spill. This was fixed in January 2014.

6 pF. It was shown, that signal over noise ratio is improved for higher gains, therefore 1.2 pF was chosen.

Fig. 2 shows as an example the signals in every channel in chip 2 (on the lower left if viewed from the chip side with DIF on top) in the first slab #2. This chip in all slabs has always the lowest noises and does not have any channel connected to more than one pixel. Therefore, here no one channel is masked.

The average number of events per channel with signals above 35 ADC counts is about 250, the statistics for all channels is shown in Fig. 3. In the following, all channels (0.9% of the total) with the statistics outside $\pm 4\sigma$ band (with $\sigma = \sqrt{N}$, N is the average statistics), shown by red lines in Fig. 3, are excluded.

For simplicity, the most probable value (MPV) of the Landau-distributed energy depositions has been estimated per channel with the simple truncated mean method described in the following. From the left, all events with signals below 40 ADC counts have been removed. From the right, 45% of the remaining statistics has been cut (the long tail of the distribution). The average of the remaining statistics gave MPV. This was done per channel, while Fig. 4 demonstrates the same method applied to the total cosmic signal summed over all channels. The truncated band is shown by the solid blue lines and the average, ie. the determined MPV position, by the solid red line. 45% number was

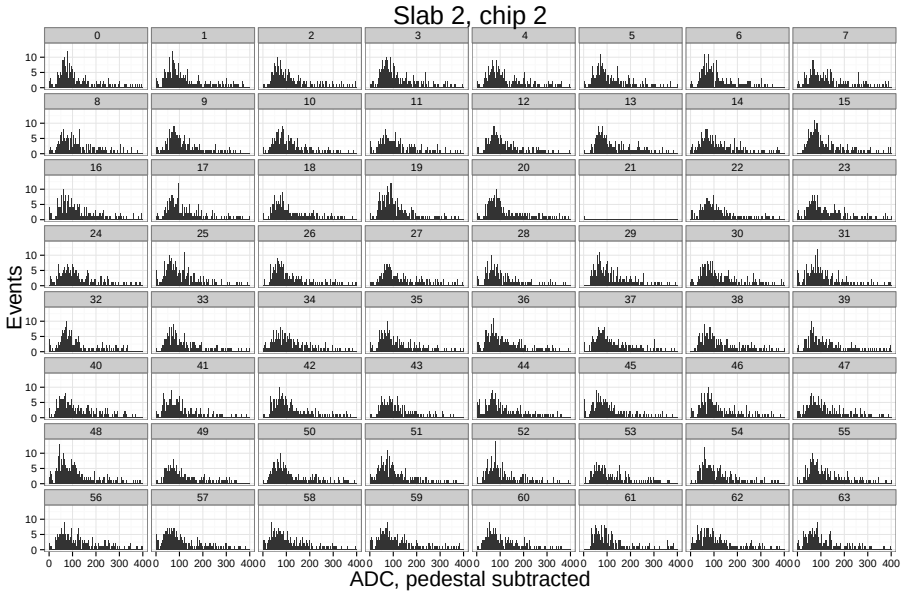

Figure 2: Slab #2, chip 2: cosmic signals in 64 channels. No one channel is masked here.

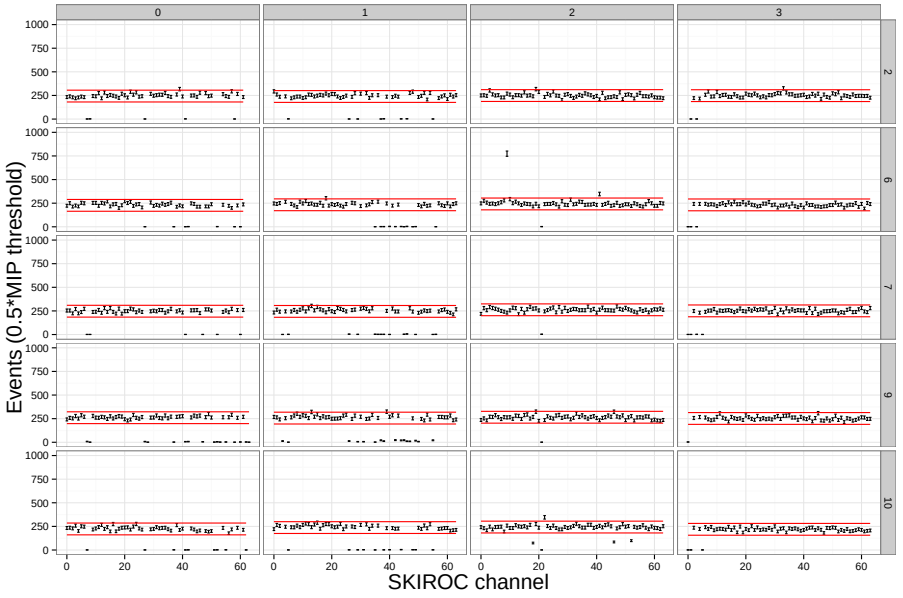

Figure 3: Per channel statistics of events with signals above 35 ADC counts (about 0.5 MIP). Red lines show $\pm 4\sigma$ statistical band.

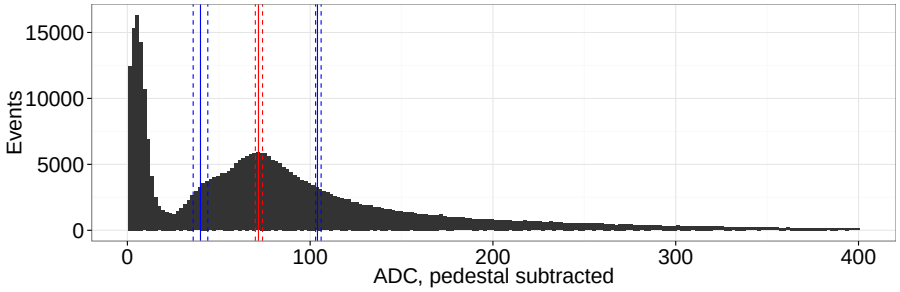

Figure 4: Sum of all cosmic signals in all channels. The blue lines show the position of the truncated band. The left blue line is fixed at 40 ADC counts. 55% of events having ADC > 40 are between the blue lines, 45% are on the right from the right line. The red line shows the position of the truncated mean over statistics between the blue lines. The dashed counterparts are obtained when the left cut is fixed at $40/1.1$ or $40 \cdot 1.1$ instead of 40.

chosen to get MPV in the right place. The truncated mean method was chosen because it is robust and sufficiently reliable. Fitting the histograms to Landau distribution modified by the cosmic particle angular spread and convolved with the resolution is more precise, but sometimes may fail to converge (especially with ~ 1000 channels). The truncated mean method looses some statistics, but always gives the result.

In principle, the truncated mean method works only if some fraction of statistics is cut from both left and right sides, while in our case on the left we apply the fixed ADC > 40 cut. This brings some bias, which should be corrected. Indeed, the cut position represented as a statistical fraction moves synchronously with MPV: eg. for higher MPVs the events tend to have higher ADC values. Eg. the position of our right cut which splits events as $0.55 : 0.45$, effectively moves to the right. The same should effectively happen with our left cut, but it is always fixed at 40. The region between 40 and the correct left cut position still contributes to the truncated mean and effectively slightly shifts it to the left. Therefore, our method tends to reduce the MPV spread between the channels: for higher MPVs there is a compensating bias to the left.

The bias may be easily corrected, however, if we assume that the shape of the spectrum is always the same, but due to gain variations it may only be stretched or squeezed. Let's approximate this shape by the cosmic signal accumulated in all channels shown in Fig. 4. This should be good enough since, as we shall see in a moment, the spread between the channels is of the order of a few percent only.

Let's assume that for one channel the gain is 10% higher than in average and stretch this shape by 10%. The left cut position stays at 40 in absolute units. If squeezed back to the original scale of Fig. 4, it will be at $40/1.1$, however, as shown by the left vertical dashed blue line. The left dashed blue

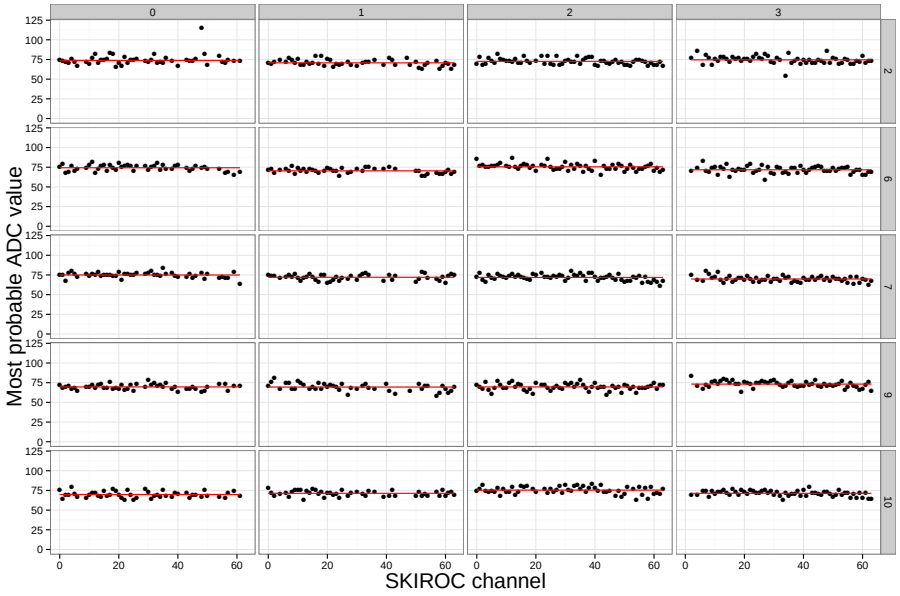

Figure 5: Most probable value (MPV) for all calibrated channels. MPV is obtained with the truncated mean method and corrected for the bias introduced by the cut ADC > 40, see the text.

line in the right pair (close to 100) shows the adjusted position of the right cut, splitting this slightly larger statistics again according to $0.55 : 0.45$. With the new cut positions the truncated mean changes by 2.7% and is shown by the left dashed red line. Note, that to represent the effect on the same Fig. 4 with its original scale, we have squeezed the spectrum by 1.1. If we again stretch the spectrum back by 10%, the truncated mean represented by the dashed red line will be higher than its solid counterpart not by 10%, as it should, but only by $10 - 2.7 = 7.3\%$. Therefore, the bias can be compensated by enhancing all deviations from the average value by $10/7.3$. For a measured truncated mean M and the average truncated mean $\overline{M}$, after compensation we arrive at

$$M_{corr} = \overline{M} + (M - \overline{M})/0.73.$$

The resulting MPV values after correction are shown in Fig. 5.

To estimate the MPV statistical error, the following method was applied. Let's again neglect a few percent differences between the gains in different channels and consider the spectrum in Fig. 4 as the average response. All statistics of events contributing to this spectrum was split randomly into samples with N events, where N is an average number of cosmic particles per channel ($N \approx 250$). The number of samples thus equals to the number of channels. The MPV in every sample was found and the MPV spread was taken as the statistical error.

	Spread, %	Stat., %	Above stat., %	Spread in physical prototype, %
All	6.1	5.1	3.3	~ 5
Within chip	5.5	5.1	2.1	
Between chips	2.9	0.7	2.8	

Table 1: The spread of calibration constants across all channels (first line), average spread within the same chip (second line) and the spread between chip averages (third line). The third column is an estimation of the statistical error obtained by random resampling of all events (described in the text). The fourth column is obtained by subtracting in quadrature the statistical spread from the total spread given in the second column.

All results are summarized in Table 1. The first three columns present, respectively, the measured MPV spread, the estimated statistical dispersion and the final estimated spread of calibration factors when the statistical spread was subtracted in quadrature. Note, that the latter may be due to both gain variations in electronics and MIP ionization variations in pixels (eg. due to slight changes in silicon thickness). The last two lines in Table 1 show the average variation between channels of the same chip and the spread between MPVs averaged over chips, respectively. The latter (2.8%) is quite close to the total spread between the channels (3.3%), indicating that electronics gain variations may be dominating.

As it was demonstrated in this section, the cosmic calibration is a perfect tool for both debugging and calibrating the detector. In total, 1080 channels were calibrated in this analysis with the statistical accuracy of about 5% per channel. The fraction of not calibrated channels may be found in Table 2.

Note, that in the presented analysis the statistics of cosmic events was severely reduced by the bug which limited the spill data taking to first 5 msec. One week of running, therefore, was required. As a further example, we discuss in the next section the calibration of slab #8 performed in January 2014, after the bug was found and fixed. The necessary cosmic statistics was accumulated in less than one day.

4 Slab #8 tests in January 2014

In 2014 LLR has sent to Research Center for Advanced Particle Physics in Kyushu University (Japan) one slab together with the full readout chain for tests. Before shipment, the setup was tested with cosmic particles and charge injection in the SKIROC chips. The cosmic data have been collected in 18 hours

	N channels	Fraction, %
Calibrated	1080	84.4
Not calibrated:		
connected to 2 or 4 pixels (masked)	120	9.4
connected to 1 pixel but still noisy (masked)	65	5.1
statistics outside $\pm 4\sigma$	12	0.9
$MPV > 100$ (outliers)	3	0.2
Total	1280	100

Table 2: Statistics of calibrated and not calibrated channels. Note, that in the next FEV9-10 versions every channel is connected to one pixel.

in January 2014 in continuous power mode. After removing 5 msec limitation, the cosmic rate reached the expected value, slightly less that 2 Hz. Compared to the running in May 2013 when the spill duration was set close to 100 msec (but only 5 msec were used), it was increased by about factor of 20. The same automatic masking and analysis code was reused for this and similar studies (written with R programming language).

The automatic procedure masked 18% of all channels. After that the noises were almost negligible. The accumulated cosmic spectra for four chips, for 64 channels in the best chip 2, the channel statistics and the obtained MPVs are shown in Figs 6-9. Due to higher statistics ($N \approx 560$ events per channel instead of ≈ 250 in the previous analysis) the statistical error was lower, 3.5%. After subtracting it in quadrature from the measured spread across all channels (5.3%), the remaining spread was found to be 4%. This is consistent with the 3.3% spread from Table 1. Again, 4% is dominated by variations between chip averages (3.5%).

One can conclude that with such a few percent non-uniformity, the silicon detector is ideal for the electromagnetic calorimeter, it is both easy to calibrate and should allow very low systematic errors. The statistical accuracy of cosmic calibration in 24 hours is 3% per channel.

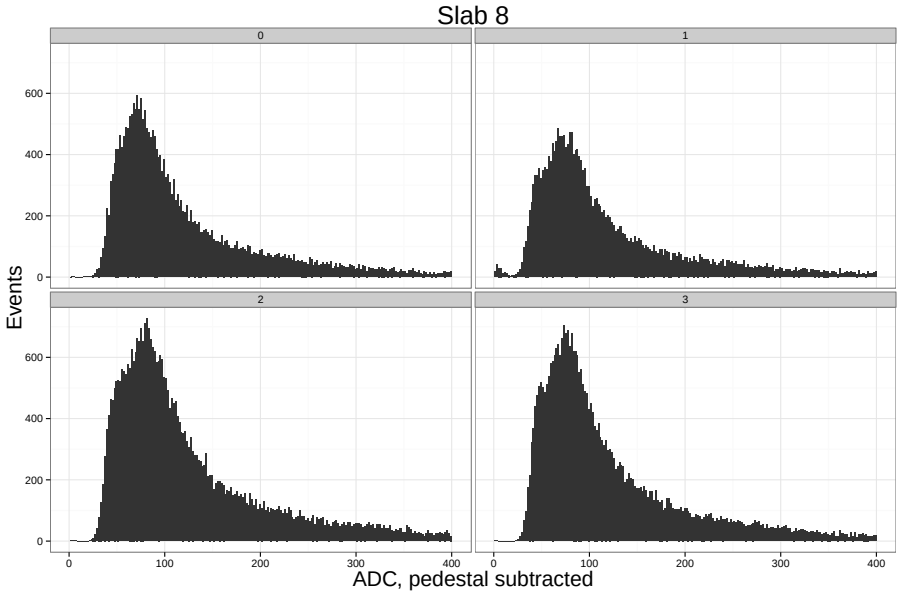

Figure 6: Accumulated during 18 hours in January 2014 cosmic signals per chip for slab #8. Pedestals are subtracted. The rate of events was slightly less than 2 Hz per slab.

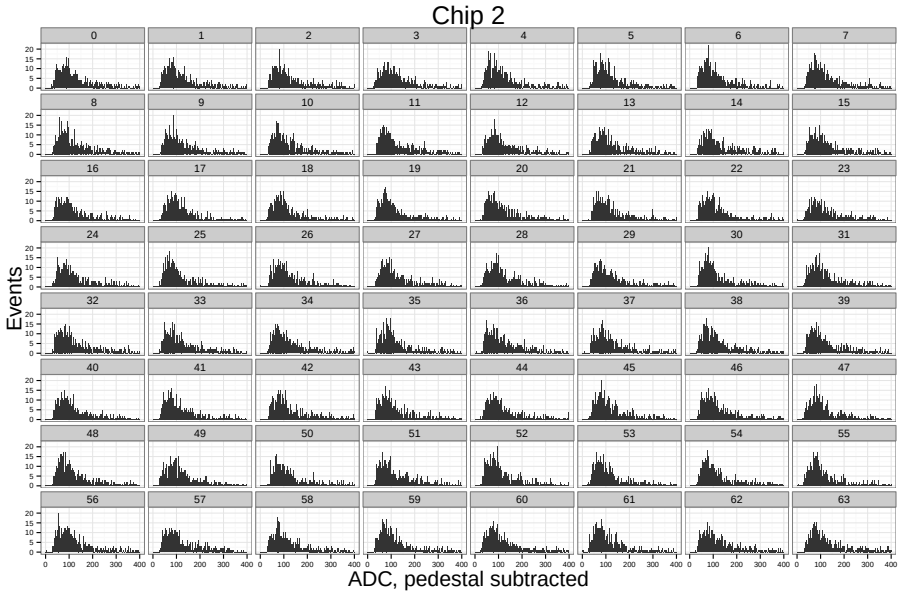

Figure 7: Slab #8, chip 2: cosmic signals in 64 channels. No one channel is masked here.

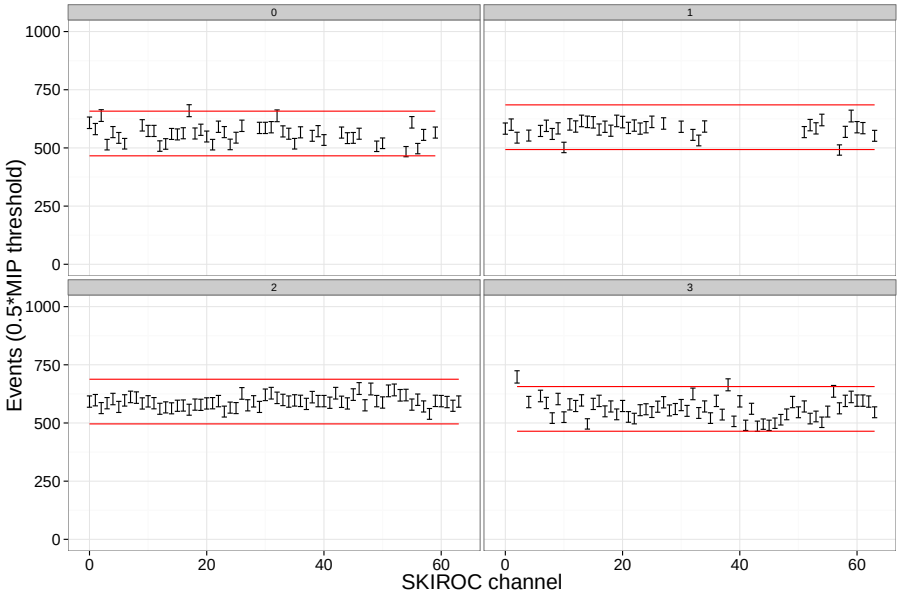

Figure 8: Per channel statistics of events in slab #8 with signals above 35 ADC counts (about 0.5 MIP). Red lines show $\pm 4\sigma$ statistical band.

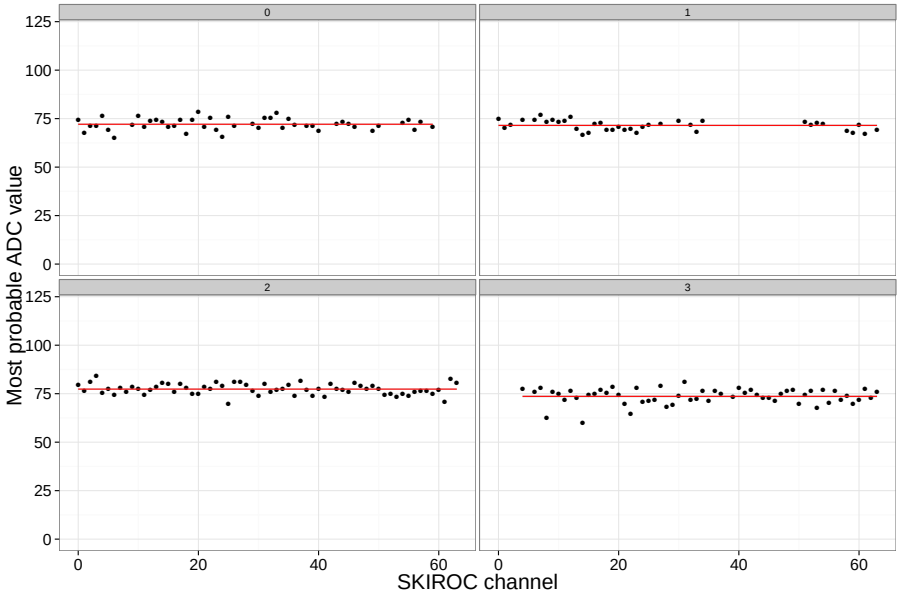

Figure 9: Most probable value (MPV) for all calibrated channels in slab #8. MPV is obtained with the truncated mean method and corrected for the bias introduced by the cut ADC > 40, see the text.